

The 10 cm Atom Probe*

J. A. Panitz

Sandia Laboratories, Albuquerque, New Mexico 87115

(Received 12 February 1973; and in final form, 16 April 1973)

A novel atom probe is described which can determine the mass-to-charge ratios of all ion species produced during a single desorption event or of individual species at several preselected crystallographic locations during each desorption event. This is accomplished without tip movement in an instrument no larger than a conventional field ion microscope by using a new channel plate photomultiplier detector. Alignment, aiming, and pulse stability problems common to all previous designs have been eliminated. Although the present mass resolution is 4 amu at $m/n = 184/3$, single isotope resolution, if desired, seems possible.

INTRODUCTION

The atom-probe field ion microscope¹⁻⁵ is a unique instrument providing the ultimate in micromass analysis of metal surfaces. Unfortunately, the atom-by-atom identification of the surface provided by the device is tedious, particularly in those metallurgical applications requiring composition analysis throughout the bulk of a specimen. Furthermore, most of the instruments discussed in the literature have been large and cumbersome, usually requiring differential pumping of the spectrometer and complicated mechanisms for moving the emitter. As a result, atom-probe investigations have been successfully undertaken by only a few individuals, the device remaining for the most part a highly specialized laboratory instrument. It is the purpose of this paper to describe a new and simple atom-probe which permits rapid, in depth species identification or the more usual atom-by-atom analysis provided by its predecessors. This has been accomplished with an instrument having a volume of less than two liters in which tip move-

ment is unnecessary and the problems of evaporation pulse stability and alignment common to all previous designs have been eliminated. Although the mass-to-charge ratios of desorbed species are still determined by a time-of-flight technique, the drift region has been made an order of magnitude shorter than that of previous instruments. This permits the entire surface of the specimen under investigation to be imaged directly at the detector, and a novel scheme allows for precise species identification at one or several preselected image spots during a single evaporation pulse without the use of a "probe hole."

PRINCIPLE OF OPERATION

The new atom-probe as shown in Fig. 1 consists of a field ion microscope with a channel plate electron multiplier assembly replacing the conventional fluorescent screen. A bias voltage $+V_A$ is applied to a stationary tip assembly of conventional design⁶ surrounded by a cylindrical electrode held at a potential $-V_C$ sufficient to establish the required imaging field. An aperture in this electrode, opposite the tip, permits ions to travel from the tip into a drift region at ground potential. Between the tip and electrode, ions are accelerated. Between the electrode and the entrance to the drift region, ions are decelerated, so that their kinetic energy within the field-free drift region is determined solely by the magnitude of the positive bias V_A . If a high voltage pulse of sufficient amplitude $-V_P$ is applied to the electrode, an atomic layer is field desorbed from the tip surface,⁷ the resulting ions traveling from the tip through the drift region to the first channel plate of the multiplier array. This is in sharp contrast to the operation of previous instruments in which the final kinetic energy of the ions produced by the desorption pulse was determined by a positive bias applied to the tip and the magnitude and duration of the desorption pulse itself.

Two modes of detection are possible in the new instrument. If the arrival of the desorbed ions is recorded by connecting the aluminized phosphor of the channel plate array directly to an oscilloscope whose sweep is initiated by the desorption pulse, the travel times of all ions striking the channel plate can be directly measured. Because of the short flight path (~ 10 cm), essentially all of the specimen is imaged on the channel plate. As a result, all of the ions produced by the desorption event are monitored at one time, permitting a rapid evaluation of species concentration over the entire surface. This is a significant departure from

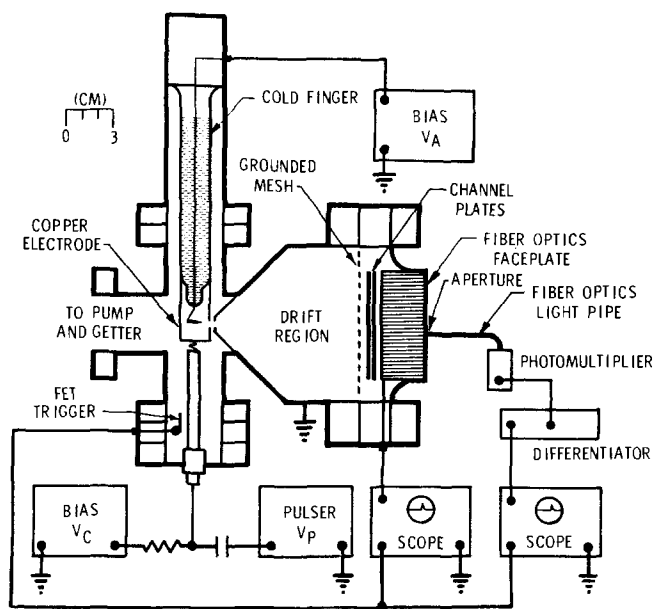


FIG. 1. The atom probe and associated electronic circuitry. Imaging is done at the detector, eliminating the need for a probe hole or a mechanism to move the specimen. The ions produced at the specimen surface are accelerated toward the copper electrode and are decelerated between the copper electrode and the entrance to the drift region. As a result, the ion energy in the drift region is determined only by the bias voltage $+V_A$. The evaporation pulse amplitude and duration are no longer important. By observing the desorption image directly, evaporation rates in vacuum can be precisely controlled, and the aiming problem of previous instruments completely eliminated.

previous atom-probe philosophy which restricted ion determination to several image spots at best.

The second mode of detection permits atom-by-atom analysis but without the necessity of tip movement and probe hole size considerations common to all previous designs. Imaging gas is introduced at a pressure of 10^{-6} Torr, producing a conventional ion image on the fluorescent screen of the multiplier array. A suitably apertured photomultiplier, external to the vacuum system, is placed over a selected image spot. Its output is differentiated and fed to the input of an oscilloscope whose sweep is triggered by the desorption pulse. Now the travel time of only those ions producing scintillations on the portion of the phosphor screen opposite the apertured photomultiplier will be recorded. If the aperture is equal in size to a single image spot, atom-by-atom analysis is possible; and if several apertured photomultipliers are used, atom-by-atom analysis can be obtained at several different locations. This provides a capability unavailable with all previous instruments in which different crystallographic locations could be examined only by moving the emitter after the evaporation pulse had altered the surface and presumably the location of adsorbates of interest.

Since the ion energy is determined solely by the dc bias applied to the tip and is not affected by the amplitude or duration of the desorption pulse, pulse requirements are noticeably relaxed over previous designs. In fact, the only important requirement is that the pulse is of sufficient amplitude to cause the desorption event and that its risetime is comparable to the uncertainty in the measurement of the ion travel time, thereby eliminating a possible source of timing inaccuracy. If the drift distance is known, the mass-to-charge ratio of detected species can be shown to be simply

$$m/n = Ct^2 \quad C \equiv (0.193/d^2)V_A, \quad (1)$$

where d is measured in m, V_A in kV, t in μsec , and m/n in amu. If V_A is held constant, the travel time for each ion species will be constant and the repetitious m/n calculations of previous atom probes can be eliminated.⁸ In practice, V_A is usually fixed at 3 or 4 kV. As the tip radius changes from successive evaporations, the bias voltage V_C is increased to maintain the required imaging field.

The choice of the drift distance, d , is a compromise. It is made as small as possible so that the divergent field-ion image occupies all of the channel plate, while being large enough so that a reasonable bias voltage will provide adequate resolution and ion travel times within the capability of a high speed oscilloscope. Obviously, if the bias voltage is too small, the ion kinetic energy will be small and external magnetic fields will affect the resulting trajectories. Fortunately, for a bias voltage of $V_A \geq 50$ V, the deflection of an ion at the channel plate due to the earth's magnetic field is negligible.

APPARATUS

The new atom probe is shown in Fig. 2. The specimen to be examined is mounted in the usual fashion at the base of a glass cold finger and surrounded by a copper cylinder to

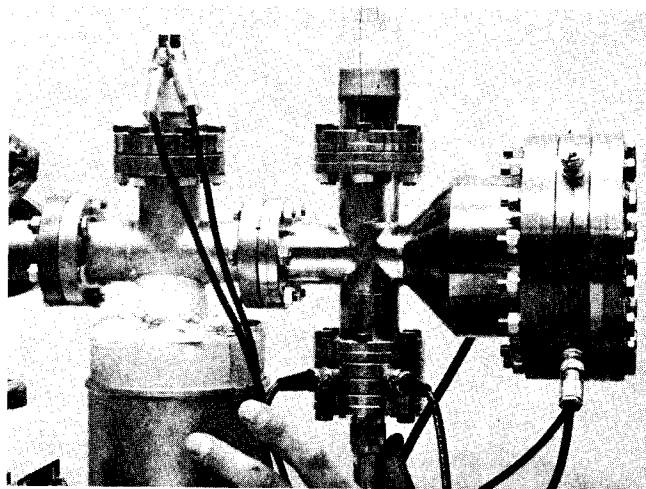


FIG. 2. The atom probe. Photomultiplier and fiber-optics light pipe have been removed for clarity. Note the use of 7 cm vacuum components.

which the negative bias and pulse voltages are applied. When liquid nitrogen is introduced into the cold finger, the copper cylinder contracts and soon reaches 78 K, enhancing image brightness by precooling the imaging gas, thereby improving thermal accommodation with the emitter.⁶ Spaced less than 2 mm away is an aperture which defines the entrance to the drift region. The entire assembly as shown is fabricated from inexpensive high vacuum components and is easily pumped to 10^{-9} Torr by a 2 cm trapped oil diffusion pump after a mild bakeout at 200°C for 2 h. A molybdenum getter cooled to 78 K keeps the pressure in the instrument at 3×10^{-9} Torr or lower for a period of several hours without pumping. A microleak valve connected between the system and a 1 liter flask of research grade helium provides the required imaging gas. The use of a channel plate detector permits imaging gas pressures of 10^{-6} Torr or less, eliminating the need for the more elaborate differentially pumped instruments previously described. Although these low pressures insure an adequate mean free path for ions between tip and detector, the imaging gas is often pumped out before field evaporation to eliminate scintillations on the channel plate screen caused by the imaging gas ions.

The evaporation pulse is supplied by a pulse generator⁹ having a pulse amplitude of 0–20 kV, a pulse width of 200 nsec, and a risetime of less than 5 nsec. The generator is manually triggered and supplies single pulses as required. Since changes in pulse amplitude or duration only affect the evaporation field and not the ion energy in the drift region, carefully terminated pulse lines are no longer a requirement for successful atom probe operation. The elimination of the severe pulse requirements is extremely important since previous work has clearly demonstrated the problems associated with less than ideal evaporation pulse waveshapes.¹⁰ To insure that a minimum and constant delay time is present between triggering the pulse generator and the start of the oscilloscope sweep, the pulse is monitored within 2 cm of the tip by an in-vacuum FET emitter follower¹¹ which provides the oscilloscope trigger. The bias voltage V_A , which determines the ion kinetic energy, is set by an ultrastable

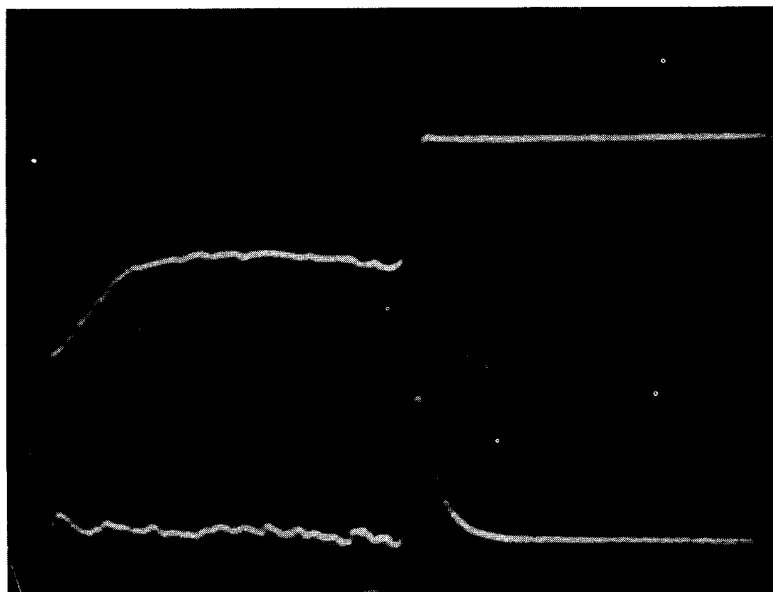


FIG. 3. Undifferentiated output of photomultiplier (upper trace), total decay time of phosphor after increase in intensity due to arrival of final ion species is approximately $1 \mu\text{sec}$; differentiated output (lower trace) 600 nsec/div. , $m/n=184/3$ (W^{3+}), $V_A=4 \text{ kV}$, $V_C=8.75$, $V_P=3 \text{ kV}$.

dc power supply¹² with 0.001% regulation and a ripple of less than 200 mV .

The detector was assembled from two 75 mm channel plates,¹³⁻¹⁵ each cut at a 5° bias and placed in a chevron configuration 3 mm from a deposited P5 phosphor screen. A grounded mesh of 90% transmission was placed in front of the input plate. With 700 V across each plate and 3 kV between the output plate and screen, a gain of 10^5 could be

obtained. Ion feedback prevented operation at higher gains, strongly suggesting that one should employ the plate configuration used in a commercially available array having lower noise at higher gains.¹⁶ The grounded mesh at the input permitted the first plate to be held at a large negative voltage so that the screen, at ground potential, could be connected to an oscilloscope. P5 phosphor was chosen because of its rapid risetime and its spectral response which almost exactly matches the RCA 4615 photomultiplier used as a scintillation detector for the single species mode, thereby maximizing over-all sensitivity.

A differentiator at the oscilloscope input extracts the fast risetime phosphor scintillation due to the arrival of desorbed ions from the longer time phosphor decay characteristic (see Fig. 3).

AIMING CONSIDERATIONS

Because the detector images the ion pattern, aiming requirements are greatly simplified over previous designs. For example, the displacement of the ion image by a change in the ratio of tip to shield potentials¹⁷ is immediately apparent (see Fig. 4); therefore, the photomultiplier can be positioned over the shifted image spot. It is this capability of selectively positioning over the *shifted* image¹⁸ which makes the electrode configuration of the present design feasible as opposed to an earlier instrument¹⁹ in which a similar pulsing technique could cause ambiguity if preselected sites were to be examined.

In addition, by photographing the image produced by the desorbed ions²⁰ at the detector (see Fig. 5), a precise position for each desorbed ion can be recorded. Using this information, single preselected atomic sites can finally be examined by placing the photomultiplier at the position of the desired desorbed ion image spot, thereby solving the fundamental aiming problem of all atom probes—the difference in position between the imaging gas and desorbed ion image. In the past, although recognized, this aiming problem has been largely ignored because of the tedious trial and error approach which had to be used to determine the correct probe hole

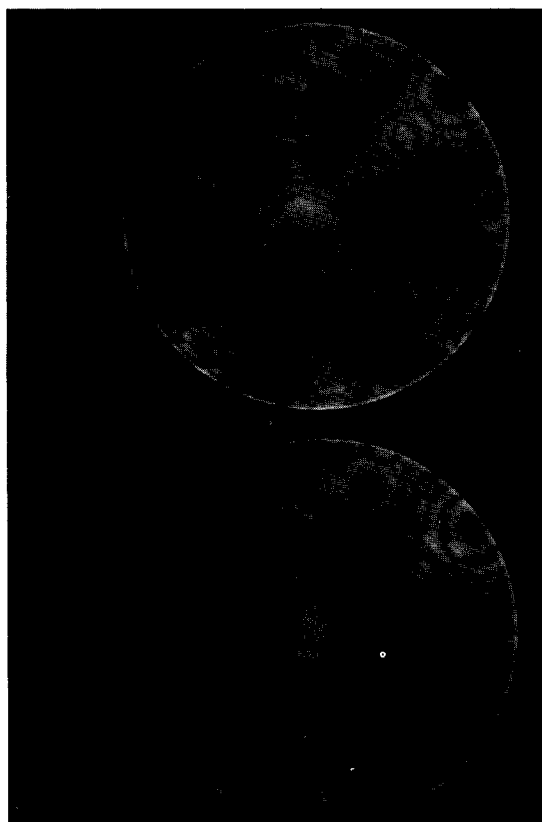


FIG. 4. Ion image at output of channel plate taken through 90% transmitting mesh. Imaging at the detector permits any number of meshes to be inserted in the ion's path since their effect can be visually determined. $6.7 \times 10^{-6} \text{ Torr He}$ (78 K), $V_A=9.39 \text{ kV}$, $V_C=0$ (upper); $V_A=5 \text{ kV}$, $V_C=4.4 \text{ kV}$ (lower).

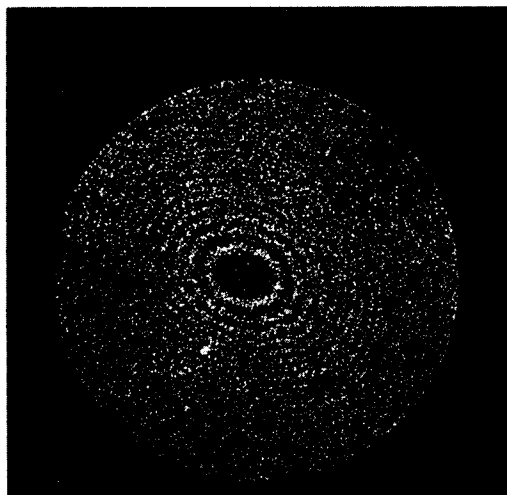


FIG. 5. Desorption image of tungsten at 78 K. $V_A=12$ kV, $V_c=0.5$ kV, $V_P=2$ kV, $P=1.3\times 10^{-9}$ Torr. P1+P5 phosphor screen. Image recorded by direct contact of Polaroid (ASA 10 000) film with fiber-optic faceplate of detector (Bendix CEMA, operated at 1700 V) V_P adjusted for gentle evaporation of 110 plane. By visually observing the desorption image, the evaporation rate in vacuum can be accurately selected. Bright area near 110 plane is a detector anomaly.

position.²¹ Often, the probe hole was made much larger than the selected image spot to insure that ions were detected and although this corrected for the uncertainty in the desorbed ion's position, it never allowed the atom probe to be used as originally intended—for the detection of a single species preselected at the discretion of the investigator.²

CALIBRATION AND RESOLUTION

Calibrating the new atom probe is somewhat easier than calibrating earlier instruments¹⁰ because the ion energy is determined only by an ultrastable dc power supply. As a result, since the drift distance can be accurately measured, the only significant uncertainty can be in the travel time measurement caused by cable, pulser, and sweep delays. This means that Eq. (1) should actually be written as

$$m/n = C(t+\delta)^2, \quad C \equiv (0.193/d^2)V_A, \quad d=0.112 \text{ m.} \quad (2)$$

One simply chooses δ , which could be positive or negative depending on the nature of the delay, so that Eq. (2) predicts the correct m/n value for a known species. Then, provided δ is a constant, Eq. (2) can be used to determine the identity of unknown species. In the present instrument $\delta = +0.091 \pm 0.005 \mu\text{sec}$ and is constant. It should be noted that the drift distance, d , in Eq. (2) is not strictly a constant but depends upon the position of the ion at the channel plate. This is due to the divergent ion trajectories between the tip and the planar grid which defines the end of the drift region. That is, an ion forming an image spot at the extreme edge of the pattern travels a longer distance than the identical ion forming an image near the center of the pattern. By placing a photomultiplier over an image spot at the center of the screen and then over an image spot at its edge, the shift in travel time for a given single species resulting from the different drift distance can be directly measured. In the present instrument this amounts to $\Delta t \approx 0.060 \mu\text{sec}$ and can accordingly limit resolution when the

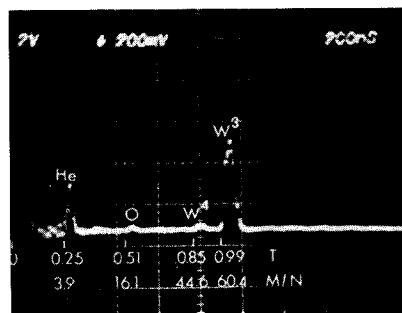


FIG. 6. Direct output from channel plate showing all species present (200 nsec/div.), $V_A=4$ kV, $V_c=8$ kV, $V_P=3$ kV, 6.7×10^{-6} He. Because peak amplitudes change by only 10–15% during successive sweeps, abundance ratios within this uncertainty can be obtained. For example, $W^{4+}/W^{3+}=0.1$.

output of the channel plate is connected directly to an oscilloscope, thereby recording the travel times of all desorbed species (see Fig. 6). Fortunately, the problem can be eliminated by using a hemispherical grid in place of the planar mesh now used. The drift distances would be the same if the tip was placed at the center of curvature of the mesh, although the distance and resulting travel times for ions between the mesh and first channel path would now depend on position. But since the nominal travel time between mesh and channel plate is small compared to the travel time in the drift region, such differences would be unimportant in calculating the mass-to-charge ratio of observed species.

The expected mass resolution in the single-atom mode at any image spot can be obtained directly from Eq. (2), noting that the only variable is the travel time t . That is,

$$\frac{\Delta(m/n)}{m/n} = \frac{2\Delta t}{(t+\delta)}.$$

Consider the result obtained by singly differentiating the output of a photomultiplier when examining several image spots of a tungsten emitter by using a large aperture in front of the photomultiplier. One finds from Fig. 7 that for $\Delta t = 0.04 \mu\text{sec}$, $t = 1.06 \mu\text{sec}$, and $\delta = +0.091$

$$\frac{\Delta(m/n)}{m/n} = 0.07$$

or

$$\Delta(m/n) = 4 \text{ amu at } m/n = 184/3.$$

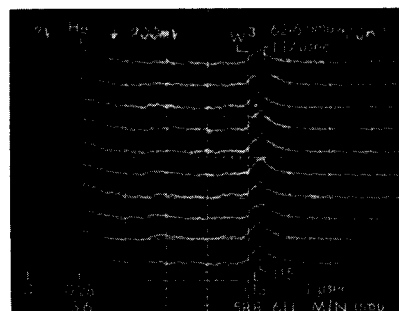


FIG. 7. Differentiated photomultiplier output, 200 nsec/div. Maximum peak separation on successive sweeps due to maximum isotope separation W^{3+} ($m/n=184/3$). $V_A=3$ kV, $V_c=7$ kV, $V_P=3$ kV, 6.7×10^{-6} He.

Although the individual isotopes cannot be resolved, the resolution is adequate for many applications. Preliminary results indicate that single isotope separation is possible if another derivative of the photomultiplier output is taken. Of course, increasing the drift distance for a given ion kinetic energy will also increase resolution. But without a lens to focus the divergent ion trajectories or a means to move the emitter with respect to the channel plates, only a small portion of the entire imaged surface could be examined at one time. If the ion energy could be reduced by setting $V_A \cong 50$ V, travel times in the microsecond range would be obtained with correspondingly improved resolution. This would be possible by replacing the present, simple electrode configuration with one that would permit a smaller ratio of tip to shield potential without image distortion.¹⁷

As with any instrument employing an electron multiplier for a detector, absolute ion abundances, or even relative ion abundances, cannot be directly inferred from the amplitudes of the ion peaks. This results from the statistical nature of the multiplication process. However, in the present instrument one observes only a 10–15% variation in the amplitude of an ion peak during successive desorption events when the entire desorbed image is monitored. Within this uncertainty the amplitude of a peak resulting from a single ion impact can be deduced by summing the amplitudes of all peaks observed during a single desorption event and dividing by the number of image spots. Assuming that one desorbed layer is produced during each desorption event, and that the detection efficiency for all species is equal, a result of 0.6 mV/single ion impact is obtained.²² Such a number is difficult to obtain with the conventional atom probe since it provides no information as to the actual number of ions which strike its detector during a single desorption event.

ACKNOWLEDGMENTS

The author wishes to thank D. W. Tipping for his assistance in various phases of instrument construction, F. E. Tentant and the scientific glass facility at Sandia Laboratories for their glass blowing expertise, and J. Abraham and L. Owens of the Bendix Corporation for advice on channel plate operation and a fiber-optics light pipe sample which coupled the photomultiplier to the ion image.

*Supported by the U. S. Atomic Energy Commission.

¹E. W. Müller and J. A. Panitz, 14th Field Emission Symposium, Washington, D.C., 1967.

²E. W. Müller, J. A. Panitz, and S. B. McLane, *Rev. Sci. Instrum.* **39**, 83 (1968).

³E. W. Müller, *Ber. d. Bunsenges.* **75**, 979 (1971).

⁴S. S. Brenner and J. T. McKinney, *Surf. Sci.* **23**, 88 (1970).

⁵S. S. Brenner and S. R. Goodman, *Scr. Metall.* **5**, 865 (1971).

⁶E. W. Müller, *Adv. Electron. Electron Phys.* **13**, 83 (1960).

⁷As in all other atom probe designs, field evaporation will continue for the duration of the applied pulse unless its nominal amplitude is carefully adjusted so that a field evaporated end-form is reached early in the pulse. The effect of continual evaporation during the applied pulse is to broaden the detected ion peaks and thereby limit resolution unless the evaporation event is terminated in a time shorter than the separation in time of the adjacent species one wishes to resolve. One therefore has two options. Either gently field evaporate to reach an end-form quickly or adjust the pulse duration to be smaller than the required time resolution.

⁸In previous instruments the ion kinetic energy was determined by a dc bias and the amplitude of the evaporation pulse. Their sum had to be increased as the tip radius increased (to maintain a constant evaporation field), requiring constant recalculation to obtain each m/n value. Since each recalculation required another accurate measurement of ion travel time for each species, data reduction time soon became excessive.

⁹Electro-Optical Instruments, Inc., Pasadena, Calif., model CU60/A.

¹⁰J. A. Panitz, S. B. McLane, and E. W. Müller, *Rev. Sci. Instrum.* **40**, 1321 (1969).

¹¹J. A. Panitz, *J. Appl. Phys.* **44**, 372 (1973).

¹²CPS, Inc., Sunnyvale, Calif., model 100R.

¹³A product of the Bendix Corp., Electro-Optical Division, Sturbridge, Mass.

¹⁴J. A. Panitz, *Rev. Sci. Instrum.* **42**, 724 (1971).

¹⁵The advantages of using stacked channel plates as a detector in a conventional atom probe were mentioned previously by E. W. Müller, S. V. Krishnaswamy, and S. B. McLane, *Rev. Sci. Instrum.* **44**, 84 (1973).

¹⁶Bendix Corp., Electro-Optical Division, Sturbridge, Mass., Chevron CEMA array. Dark current count rate less than 10 counts/sec/cm² at gains greater than 10⁶.

¹⁷The ratio of tip to shield potential is restricted by the simple electrode configuration described when atom-by-atom probing is being conducted. For the present instrument, if $V_A < 0.1 (V_C + V_P)$, severe image distortion results and single atomic sites are no longer distinguishable.

¹⁸In practice, the shield potential during imaging is made as close as possible to $(V_C + V_P)$. This permits the extent of the image shift by the subsequent evaporation pulse to be seen. The detector is positioned over the shifted image spot, the shield potential reduced to V_C , and the desorption pulse, V_P , applied.

¹⁹S. S. Brenner and J. T. McKinney, *Appl. Phys. Lett.* **13**, 29 (1968).

²⁰A desorption field-ion microscope using a single channel plate and an image intensifier was recently described by R. J. Walko and E. W. Müller, *Phys. Status Solidi A* **9**, K9 (1972).

²¹J. A. Panitz, Ph.D. thesis, The Pennsylvania State University, 1969.

²²This number may be too large since the occurrence of possible spurious "after pulses" produced by ion feedback in the multiplier array has been neglected. This problem was recently considered in detail by S. S. Brenner and J. T. McKinney, *Rev. Sci. Instrum.* **43**, 1264 (1972).